Available online at www.sciencedirect.com

SciVerse ScienceDirect

Physics Procedia 27 (2012) 100 – 103

Physics Procedia

ISS2011

Investigation of flux turbulence in iron-based superconductors

Shyam Mohan[a], Tatsuro Ishibashi[a], Yasuyuki Nakajima[a,b], Yuji Tsuchiya[a], Tsuyoshi Tamegai[a,b*]

[a]*Department of Applied Physics, University of Tokyo, 7-3-1 Hongo, Bunkyo-ku,Tokyo 113-8656, Japan*
[b]*JSTTransformative Research on Iron Pnictides (TRIP), 7-3-1 Hongo, Bunkyo-ku,Tokyo 113-8656, Japan*

Abstract

We explore the magnetic flux penetration in single crystals of the 122-type iron-based superconductors after remagnetization using magneto-optical imaging. We find evidence for turbulence at the boundary between vortices and antivortices. The turbulenceis characterized by increased fingering of the flux front.Moreover, steps in local magnetic induction are observed at the flux boundary. Our results show that flux turbulence is observed even for low-anisotropy type-II superconductors and is not confined to the cuprates.

Keywords: Iron-based superconductor; remganetization; flux turbulence

1. Introduction

Magnetic flux penetration in type-II superconductors has been widely studied using magneto-optical (MO) imaging [1].The expected Bean critical state has been observed in the vast majority of samples. However some superconductors exhibit flux penetration patterns that are vastly different from the critical state. Prominent examples of these are the development of flux turbulence and dendritic avalanches [1]. Dendritic avalanches have been observed in thin films of many superconductors and are broadly understood within the framework of a thermomagnetic instability in the vortex state [2,3]. On the other hand, flux turbulence has been observed only in single crystals of the 123-type high temperature cuprate superconductors (HTC) upon remagnetization [4-9]. The turbulence manifests as a fingering instability at the flux-antiflux boundary. The mechanism that causes turbulence is attributed to underlying crystal anisotropy and/or thermal effects arising from flux-antiflux annihilation [8,10].

Experimentally the turbulence is observed in crystals with different critical current densities and moderate anisotropy [5]. Also, the turbulence is limited to specific temperature windows [4,5]. It has been suggested that flux turbulence may be present in all remagnetized type-II superconductors [9]. Motivated by this, we investigate here the effect of remagnetization in the vortex state of the 122-type iron based superconductors (IBS) using MO imaging. Our studies are also motivated by many similarities in the bulk vortex-state properties of the 122-type IBS with 123-type HTC [11]. Towards this objective we study two different superconductors derived from the same parent compound $BaFe_2As_2$: electron-doped $Ba(Fe_{1-x}Co_x)_2As_2$ and isovalent-doped $Ba(Fe_{1-x}Ru_x)_2As_2$.

* Corresponding author. Tel.: +81-3-5841-6846 ; fax: +81-3-5841-6846 .
E-mail address: tamegai@ap.t.u-tokyo.ac.jp .

1875-3892 © 2012 Published by Elsevier B.V. Selection and/or peer-review under responsibility of ISS Program Committee
Open access under CC BY-NC-ND license. doi:10.1016/j.phpro.2012.03.420

2. Experiments

Single crystals of optimally-doped $Ba(Fe_{0.925}Co_{0.075})_2As_2$ and under-doped $Ba(Fe_{0.725}Ru_{0.275})_2As_2$ were made using a self-flux method [12-14].The starting materials were placed in an alumina crucible and heated to 1150^{o}C after sealing in quartz tubes under vacuum. Subsequently they were cooled slowly (1.5 ^{o}C/hr) to 800^{o}C, following which the furnace was switched off to allow rapid cooling to room temperature. Shiny single crystals were separated from the flux by mechanical fracture. The extracted single crystals were magnetically characterized using a SQUID magnetometer (Quantum Design). The critical temperatures T_c and critical current densities J_c (extracted from magnetization hysteresis loops) of the crystal batches are given in Table 1. The MO imaging was performed in a flow-type helium cryostat (Oxford). The crystals were glued to a copper sample holder and a Bi-doped garnet film placed above the sample actsas an indicator to observe Faraday rotation. The magnetic field was applied perpendicular to the *ab* plane of the crystals. There magnetization was performed using the following protocol: The sample was field-cooled in -300 Oe from above T_c to the measurement temperature. After waiting for temperature stability, the polarity of the external field was switched to positive. Subsequently a sequence of 10 MO images was captured with a CCD exposure time of 50 ms.

Table 1. Sample specifications

Sample	$Ba(Fe_{0.925}Co_{0.075})_2As_2$	$Ba(Fe_{0.725}Ru_{0.275})_2As_2$
T_c(K)	24	18
J_c(10^5 A/cm^2)	~8	~4
Dimensions (μm^3)	~530×460×30	~560×250×32
Anisotropy	~3	~2

3. Results and discussion

Figures 1 (a)-(c) show MO images captured at 20 K (T/T_c = 0.83) in $Ba(Fe_{0.925}Co_{0.075})_2As_2$ after remagnetization to 100, 150, and 200 Oe, respectively. Here dark and brightregions refer to positive and negative values ofthe axial magnetic induction B_z arising from the remagnetized and virgin fields, respectively, and the boundary between themis the remagnetization flux front. The sample edges can be identified bythe bright outlineformed by concentration of the expelled flux. At these elevated temperatures the reversed flux has already progressed well away from the edges at 100 Oe (Fig 1(a)). The striking observation is the undulating nature of the remagnetization flux front with vastly different nature of fingering at different edges. Moreover, the front patterns have weak resemblance to the virgin magnetization patterns. With increasing reversed fields (Fig 1(b)-(c)) the remagnetization flux front moves deeper into the sample with some flux fingers penetrating faster than others.At higher fields the fronts become smoother before they finally collapse at the sample center. We believe these observations constitute the main features of the flux turbulence exhibited in this crystal. The turbulent features in the flux front propagation are observed down to the lowest measured temperature 5 K (T/T_c = 0.21).

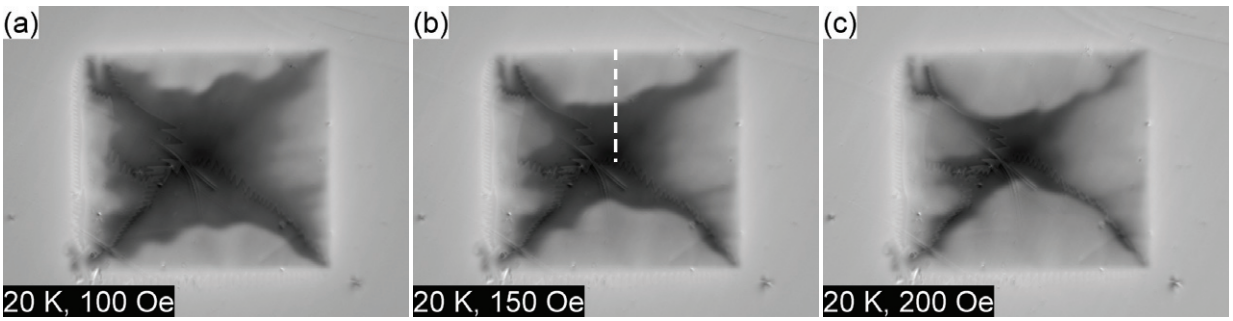

Fig. 1. MO images after remagnetization in $Ba(Fe_{0.925}Co_{0.075})_2As_2$ crystal at 20 K with reversed field of (a) 100 Oe; (b) 150 Oe; and (c) 200 Oe.

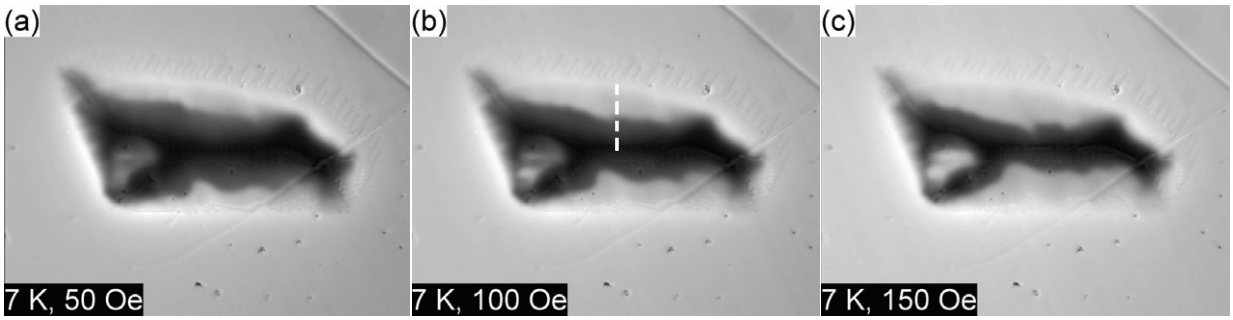

Fig. 2. MO images after remagnetization in $Ba(Fe_{0.725}Ru_{0.275})_2As_2$ crystal at 7 K with reversed field of (a) 50 Oe; (b) 100 Oe; and (c) 150 Oe.

Figures 2 (a)-(c) show remagnetization MO images 7 K ($T/T_c = 0.39$) in isovalent-doped $Ba(Fe_{0.725}Ru_{0.275})_2As_2$ with reversed fields of 50, 100, and 150Oe, respectively. The premature flux penetration close to the bottom of the left-edge is due to a weak pinning region relative to the rest of the sample. In this sample the effects of flux remagnetization are not as prominent as in $Ba(Fe_{0.925}Co_{0.075})_2As_2$. While the skeleton of the reversed front patterns resemblethat of virgin magnetization patterns, the effect of turbulence can be identified from the enhanced nature of flux fingering. In contrast to the observations in $Ba(Fe_{0.925}Co_{0.075})_2As_2$, at higher fields the fronts sustain the finger-like patterns. The temperature window of the turbulent features in the flux front propagation stretches from 5 K ($T/T_c = 0.28$) to 10 K ($T/T_c = 0.56$) which is a considerably narrow range than in $Ba(Fe_{0.925}Co_{0.075})_2As_2$.

More insight into the nature of turbulence is obtained by analyzing the local magnetic induction profiles. Via calibration, the intensity values in an MO image can be converted to the axial component B_z of the magnetic induction of the sample. Figures 3 (a) and (b) show the B_z profiles in crystals of $Ba(Fe_{0.925}Co_{0.075})_2As_2$ and $Ba(Fe_{0.725}Ru_{0.275})_2As_2$, respectively, across the dashed lines in Figs 1(b) and 2(b). The profiles are obtained from the top sample edge ($x = 0$) to the sample center. The negative B_z values at the sample interior correspond to the initial flux due to field cooling procedure (-300 Oe). Near the edges the positive fields correspond to the reversed flux entering the sample. At the boundary between flux and antiflux ($B_z = 0$) steps in magnetic induction are clearly observed in both samples. In $Ba(Fe_{0.925}Co_{0.075})_2As_2$ the steps are sharp and are associated with hump-like features on either ends. In comparison, the $Ba(Fe_{0.725}Ru_{0.275})_2As_2$ crystal has more smooth features. Such induction steps at the flux boundary have been observed earlier in single crystals of YBa_2Cu_3O that exhibit turbulence. The steps arise from the concentration of excess currents at the flux front that sustain closed vortex loops. These vortex entities are called “Meissner holes” due to the presence ofsurface-like screening currents at the flux boundary.

Considering that anisotropy appears to be an important ingredient for an explanation of turbulence [8], the fact that the anisotropy in our samples (cf. Table 1) is half of the 123-type HTC has important implications. Also, our results point to sample-specific temperature windows for the observation of the flux turbulence which agrees well with earlier observations [4,5].Taken together these observations reinforce that the physical mechanism that causes turbulence has contributions from both crystal anisotropy and thermal effects.

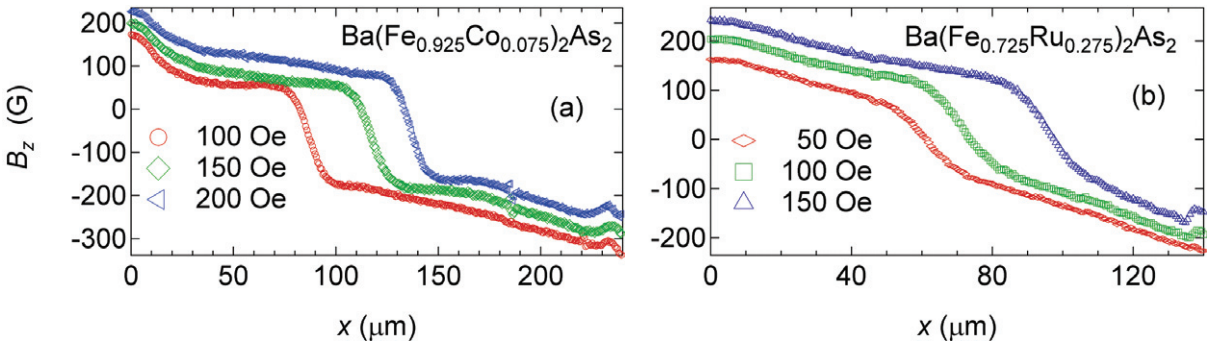

Fig. 3. Magnetic induction profiles after remagnetization in (a) $Ba(Fe_{0.925}Ru_{0.075})_2As_2$ crystal at 20 K; and (b) $Ba(Fe_{0.725}Ru_{0.275})_2As_2$ crystal at 7 K.

Our observations of the flux turbulence in single crystals of two different 122-type IBS clearly demonstrate that the turbulent flux dynamics at the remagnetized flux boundary is not limited to the 123-type HTC.

Conclusion

We have investigated the nature of flux penetration in single crystals of doped $Ba(Fe_{0.925}Co_{0.075})_2As_2$ and under-doped $Ba(Fe_{0.725}Ru_{0.275})_2As_2$ after remagnetization. The boundary between vortices and anti-vortices exhibit increased undulations and fingering. Accompanying this turbulent feature steps in local magnetic induction are also observed. Our results demonstrate that flux turbulence is also observed in low-anisotropy materials and is not confined to the 123-type HTC.

Acknowledgements

Shyam Mohan acknowledges the Japan Society for the Promotion of Science (JSPS) for a Foreign Postdoctoral Fellowship.

References

[1] Jooss CJ, Albrecht J, Kuhn H, Leonhardt S,Kronmuller H.Magneto-optical studies of current distributions in high-T_c superconductors.*Rep ProgPhys* 2002;65:651-788.
[2] Duran CA, Gammel PL, Miller RE, Bishop DJ. Observation of magnetic-field penetration via dendritic growth in superconducting niobium films.*Phys RevB* 1995;52:75-8.
[3] Johansen TH, Baziljevich M, Shantsev DV, Goa PV, Galperin YM, Kang WN, Kim HJ, Choi EM, Kim MS, Lee SI, Dendritic magnetic instability in superconducting MgB_2 films. *EurophysLett* 2002;59:599-605.
[4] Vlasko-Vlasov VK, Welp U, Crabtree GW, Gunter D, Kabanov V,Nikitenko VI. Meissner holes in superconductors.*Phys RevB*1997;56:5622-30.
[5] Frello T, Baziljevich M, Johansen T, Andersen NH, Wolf T, Koblischka MR. Flux turbulence in $NdBa_2Cu_3O_6$.*Phys RevB*1999;59:R6639-42.
[6] Uspenskaya LS, Naumenko IG, Zhokhov AA. Influence of twin structure on flux turbulence near the front of vortex annihilation. *PhysicaC* 2004;402:188-95.
[7] Vlasko-Vlasov VK, Welp U, Crabtree GW, Gunter D, Kabanov V, Nikitenko VI,Paulius LM. Meissner holes and turbulent structures in unidirectional fields.*Phys RevB*1998;58:3446-56.
[8] Fisher LM, Bobyl A, Johansen TH, Rakhmanov AV, Yampol'skii VA, Bondarenko AV, Obolenskii MA. Anisotropic origin of the bending instability of the flux-antiflux interface in type-II superconductors.*Phys RevLett*2004;92:037002-1-4.
[9] Voloshin IF, Kalinov AV, Fisher LM,Yampol'skii VA, Bobyl A, Johansen TH. Development of macroturbulent instability in a YBCO single crystals.*Low Temp Phys*2010;35:627-31.
[10] Bass F, Shapiro BY, Shvarster M. Corrugation flux front instability in type-II superconductors. *PhysRevLett*1998;80: 2441-44.
[11] Prozorov R, Ni N, Tanatar MA, Kogan VG, Gordon RT, Martin Cet al.Vortex phase diagram of $Ba(Fe_{0.93}Co_{0.07})_2As_2$ single crystals. *Phys RevB*2008;78:224506-1-9.
[12] Nakajima Y, Taen T,Tamegai T. Possible superconductivity above 25 K in single-crystalline Co-doped $BaFe_2As_2$.*J PhysSocJpn*2009 ;78:023702-1-4.
[13] Rullier-Albenque F, Colson D, Forget A, Thuery P, Poissonnet S. Hole and electron contributions to the transport properties of $Ba(Fe_{1-x}Ru_x)_2As_2$ single crystals. *Phys RevB*2008;81:224503-1-7.
[14] Thaler A, Ni N, Kracher A, Yan JQ, Budko SL, Canfield PC. Physical and magnetic properties of $Ba(Fe_{1-x}Ru_x)_2As_2$ single crystals. *Phys RevB*2008;82:014534-1-7.